MOLECULAR AND CELLULAR BIOLOGY, Nov. 2005, p. 10071–10078 Vol. 25, No. 22
0270-7306/05/$08.00+0 doi:10.1128/MCB.25.22.10071–10078.2005

Snm1-Deficient Mice Exhibit Accelerated Tumorigenesis and Susceptibility to Infection‡

Shamima Ahkter,[1] Christopher T. Richie,[1]† Nianxiang Zhang,[1] Richard R. Behringer,[1] Chengming Zhu,[2] and Randy J. Legerski[1]*

Department of Molecular Genetics[1] and Department of Immunology,[2] The University of Texas M. D. Anderson Cancer Center, 1515 Holcombe Boulevard, Houston, Texas 77030

Received 17 June 2005/Returned for modification 20 July 2005/Accepted 21 August 2005

The eukaryotic *SNM1* gene family has been implicated in a number of cellular pathways, including repair of DNA interstrand cross-links, involvement in VDJ recombination, repair of DNA double-strand breaks, and participation in cell cycle checkpoint pathways. In particular, mammalian *SNM1* has been shown to be required in a mitotic checkpoint that causes arrest of cells in prophase prior to chromosome condensation in response to spindle poisons. Here, we report on the phenotype of a knockout of *Snm1* in the mouse. *Snm1*$^{-/-}$ mice are viable and fertile but exhibit a complex phenotype. Both homozygous and heterozygous mice show a decline in survival compared to wild-type littermates. In homozygous mutant males, this reduction in survival is principally due to bacterial infections in the preputial and mandibular glands and to a lesser extent to tumorigenesis, while in homozygous and heterozygous females, it is due almost solely to tumorigenesis. The high incidence of bacterial infections in the homozygous mutant males suggests an immune dysfunction; however, examinations of T- and B-cell development and immunoglobulin class switching did not reveal a defect in these pathways. Crossing of *Snm1* mutant mice with a *Trp53* null mutant resulted in an increase in mortality and a restriction of the tumor type to lymphomas, particularly those of the thymus. Taken together, these findings demonstrate that *Snm1* is a tumor suppressor in mice that in addition has a role in immunity.

The *SNM1* gene family is represented by five mammalian members including *SNM1*, *SNM1B*, *Artemis*, *ELAC2*, and *CPSF73* (9, 13, 29). The commonality among these genes is the SNM1 domain, which contains a metallo-β-lactamase fold and an appended β-CASP sequence (4, 19). The β-CASP domain is predicted to function as a nucleic acid binding domain, and the metallo-β-lactamase fold has been shown to possess DNA endonuclease activity upon interaction between Artemis and the DNA-dependent protein kinase catalytic subunit (16). Outside of the SNM1 domain, there is no significant sequence homology between the five mammalian *SNM1* family members. At least two of these family members, *Artemis* and *ELAC2*, have been implicated as tumor suppressors. *Artemis* mutations in human patients result in a severe combined immunodeficiency (SCID) syndrome in which both T and B cells fail to mature (19). In addition, Artemis-deficient cell lines are sensitive to ionizing radiation (IR) (6, 20, 21), which has been attributed to both defects in the double-strand break (DSB) repair pathway of nonhomologous end joining (15, 16, 22) and cell cycle checkpoint signaling (33). The SCID and IR-sensitive phenotypes have been reconstructed in a knockout of *Artemis* in the mouse, and in addition, when combined with *Trp53* deficiency, *Artemis* was revealed to have tumor suppressor activity (24, 25). A second SNM1 family member, *ELAC2*, has been implicated in prostate cancer susceptibility in humans (29), although this conclusion has proven to be controversial (27).

In budding yeast, the single *SNM1* gene is involved in mediating resistance to interstrand cross-linking drugs, such as nitrogen mustard or mitomycin C (MMC), but not to other forms of DNA damage (10, 26). The yeast protein has also been shown to possess exonuclease activity (14) and appears to function in the repair of DNA DSBs that occur during processing of interstrand cross-links (2, 17). However, the function of mammalian Snm1 seems quite distinct from that of the yeast protein. While it has been shown that human Snm1 localizes to sites of DSBs after exposure of cells to either IR or cross-linking agents (23), *Snm1*-deficient cells exhibited no hypersensitivity to IR and only minor hypersensitivity to MMC (9). Thus, the function of Snm1 at sites of DSBs remains unclear. In addition, our recent findings have demonstrated that Snm1 is involved in a mitotic cell cycle checkpoint that arrests cells in prophase in response to spindle poisons, such as nocodazole and taxol (1). This checkpoint appears to correspond to the pathway that was originally discovered and found defective in *Chfr*-deficient cells (28). Consistent with a defect in the prophase checkpoint, both *Snm1*- and *Chfr*-deficient cells are highly hypersensitive to spindle poisons.

In this report, we describe the phenotype of mice in which *Snm1* has been disrupted by gene targeting. *Snm1*$^{-/-}$ mice are viable and fertile but exhibit decreased long-term survival compared to wild-type littermates. The two identified causes of this

* Corresponding author. Mailing address: Department of Molecular Genetics, The University of Texas M.D. Anderson Cancer Center, 1515 Holcombe Boulevard, Houston, TX 77030. Phone: (713) 792-8941. Fax: (713) 834-6319. E-mail: rlegersk@mdanderson.org.

† Present address: National Institute of Diabetes and Digestive and Kidney Diseases, National Institutes of Health, Bethesda, Md.

‡ Supplemental data for this article may be found at http://mcb.asm.org/.

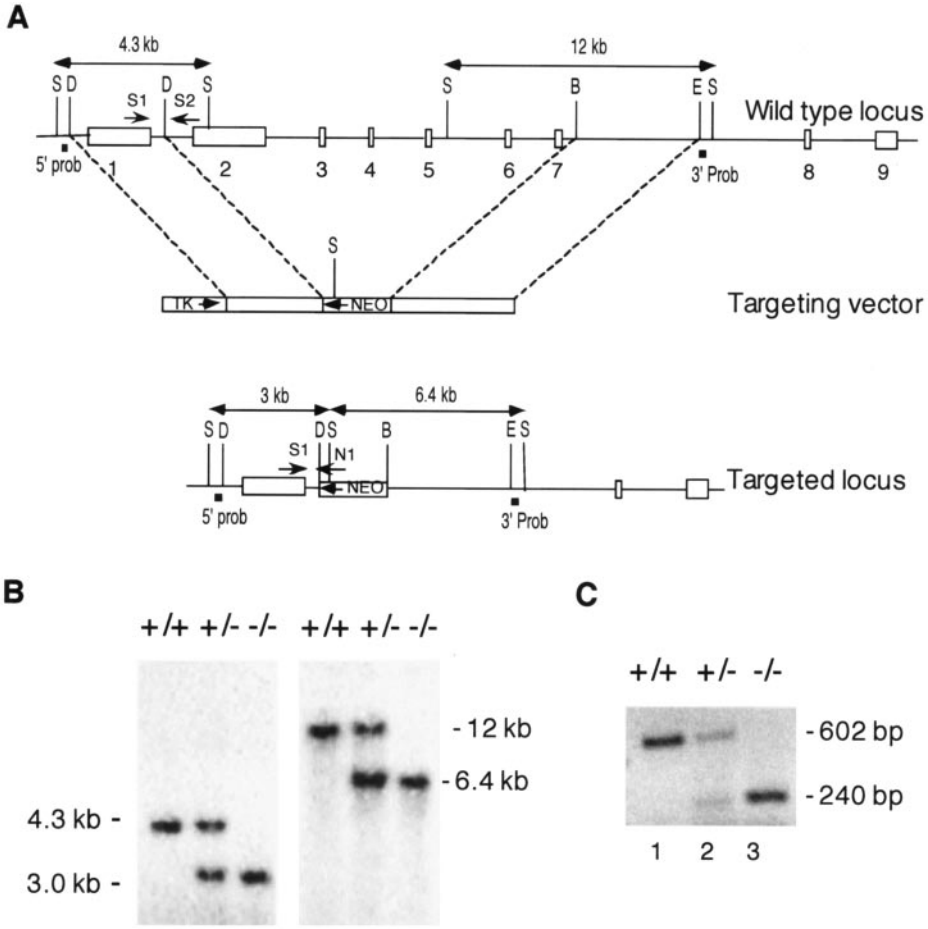

FIG. 1. Disruption of *Snm1* in the mouse by gene targeting and genotype of knockout mice. (A) Schematic representations of mouse *Snm1* locus (top) and the *Snm1* targeting vector (middle). Solid boxes denote exons, with 5′ ends to the left. D (DraI), B (BstZ171), E (EcoRI), and S (SstI), restriction enzyme sites used for analyses of the targeted deletion. Prob, probe. (B) Southern blot analysis of tail DNA from F_2 animals. The sizes of SstI fragments are indicated. Genomic DNA digested with SstI and hybridized with the 5′ probe yielded fragments of 4.3 and 3 kb in the wild-type and targeted locus, respectively (left). Hybridization with the 3′ probe yielded fragments of 12 and 6.4 kb in the wild-type and targeted locus, respectively (right). (C) Multiplex PCR genotype analysis with primer pair S1/S2 (lanes 1 and 2), which results in a 602-bp product in the wild-type allele, and with primer pair S1/N1 (lanes 2 and 3), which resulted in a 240-bp product in the targeted allele.

decreased survival are accelerated tumorigenesis and susceptibility to infection.

MATERIALS AND METHODS

Generation of *Snm1* mutant ES cells and mice. A mouse *Snm1* cDNA clone (IMAGE clone identification no. 533047) was used to screen a lambda phage mouse (129/SvEv) genomic library to obtain a fragment of the *Snm1* locus. The *Snm1* targeting construct was designed to replace exons 2 to 7 with a *loxP*-flanked PGK*neo*bpA cassette in the opposite transcriptional orientation. Gene targeting in AB1 embryonic stem (ES) cells and microinjection of targeted clones into C57BL/6J blastocysts were performed as described previously (11). Targeted recombinants were verified by Southern blot analysis using 5′ and 3′ external probes and by PCR analysis. The sequences of PCR primers were as follows: S1, 5′-CATAGAAAATTCCCCTTGGACTATG; S2, 5′-GCCAATGCATCCGAG GGGCTG; N1, 5′-AGCAAGGGGGAGGATTGGGAAGACA.

Generation of *Snm1*$^{-/-}$ *Trp53*$^{-/-}$ mice. *Snm1*$^{-/-}$ mice were crossed to *Trp53*$^{-/-}$ mice (129/C57BL; kindly provided by Guillermina Lozano) to generate *Snm1*$^{+/-}$ *Trp53*$^{+/-}$ mice, which were then bred to generate all cohort mice. Genotyping for *Trp53* was performed by PCR as described previously (12). The mice were monitored for 1 year after birth without any treatment.

Mouse handling. All mice were maintained according to NIH guidelines and an approved Animal Care and Use Committee protocol. They were maintained in a conventional specific-pathogen-free facility. The mice were regularly monitored and were sacrificed when they were moribund or when they showed signs of chronic progressive diseases.

Pathology. A complete necropsy was performed on mice that were found shortly after death, that were sacrificed because they had a tumor burden that was 10% of their body weight, that were moribund, or that displayed poor body condition. Also, randomly selected age-matched wild-type, heterozygous, and homozygous mutant mice were subjected to necropsy for phenotypic comparisons. All organs were collected and fixed with 10% phosphate-buffered formalin and stored until they were processed for histology. A portion of each organ was embedded in paraffin, sectioned, and stained with hematoxylin and eosin. Tissues were analyzed by light microscopy.

Lymphocyte analyses and CSR assays. Single-cell suspensions were prepared from thymus, spleen, bone marrow, and lymph nodes of 5- to 12-week-old mice according to a standard protocol. The cells were stained with various antibodies conjugated with fluorescein isothiocyanate (FITC) (CD8, CD43, immunoglobulin G1 [IgG1], and IgG2b), phycoerythrin (PE) (CD4 and B220), and allophycocyanin (CD3 and IgM). All antibodies were purchased from PharMingen. Fluorescence-activated cell sorter (FACS) analyses were performed using a FACSCalibur, and the results were analyzed by Cellquest (BD Biosciences). For class switch recombination (CSR), mouse sera were collected from wild-type and mutant mice, and levels of IgL, IgM, and IgG subclasses and IgA were detected by flow cytometry in a FITC and R-PE-based bead assay (SouthernBiotech). In

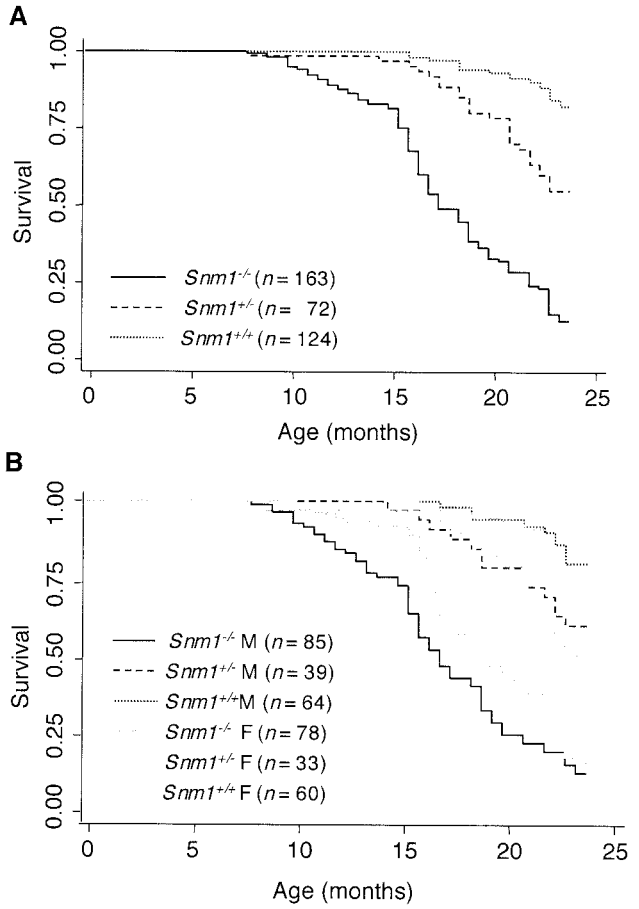

FIG. 2. Survival of *Snm1*$^{-/-}$ mice. (A) Increased mortality in *Snm1* mice shown by Kaplan-Meier analysis. *Snm1*$^{-/-}$, *Snm1*$^{+/-}$, and *Snm1*$^{+/+}$ animals were observed for 24 months. (B) Kaplan-Meier analysis showing survival by gender and genotype of *Snm1*$^{-/-}$ male, *Snm1*$^{+/-}$ male, *Snm1*$^{+/+}$ male, *Snm1*$^{-/-}$ female, *Snm1*$^{+/-}$ female, and *Snm1*$^{+/+}$ female cohort mice versus age in months.

addition, splenic B cells were also collected from wild-type and mutant mice and cultured with appropriate stimulants and cytokines to assay for class switch recombination (18).

Genotoxicity survival assays. *Snm1*$^{+/+}$ and *Snm1*$^{-/-}$ mouse embryonic fibroblasts (MEFs) were derived from 13.5-day poistcoitus embryos and cultured as described previously (1). For colonogenic survival studies, MEFs were exposed to different doses of MMC for 1 h, washed with 1× phosphate-buffered saline three times, and subsequently cultured in regular media. MEFs were also exposed to various doses of IR. For both experiments, colonies were counted 9 days later after being stained with trypan blue.

For whole-animal experiments, 9-week-old *Snm1*$^{+/+}$ and *Snm1*$^{-/-}$ mice were exposed to 7.5 Gy IR. For studies with taxol (Mead Jonson), 15-week-old *Snm1*$^{+/+}$ and *Snm1*$^{-/-}$ mice were injected with the drug at 15 mg/kg of body weight. For both studies, the mice were monitored every day until they died or exhibited morbidity.

Proliferation assay. To monitor proliferation, cells were maintained on a defined 3-day passage schedule by plating 3×10^5 cells (3T3 protocol) in 60-mm dishes as described previously (30). The cells were counted at each passage, and the total number was calculated prior to replating. Growth rates at passages 2, 5, 10, and 15 were determined by plating replicate cultures of 2.5×10^4 cells in 35-mm dishes; duplicate cultures were harvested every day thereafter, and the cells were counted.

RESULTS

***Snm1* mice exhibit decreased survival due to tumorigenesis and infections.** To investigate the function of *Snm1*, we generated mice with a homozygous deletion by targeted disruption in mouse ES cells. The targeting strategy was planned to delete exons 2 through 7, which would eliminate over 75% of the *Snm1* coding region (Fig. 1A). The human and mouse *Snm1* genes possess an unusually long 5′ untranslated region, which contains an internal ribosome entry site that regulates *Snm1* expression as a function of the cell cycle by up regulation during mitosis (32). The start of translation occurs approximately one-third of the distance from the 3′ end of exon 1. Three targeted ES cell lines were identified, and two of these were used for blastocyst injection and generation of gene-targeted mice. The genotype analyses of one of these strains are shown (Fig. 1B and C). The *Snm1*$^{-/-}$ mice were born at

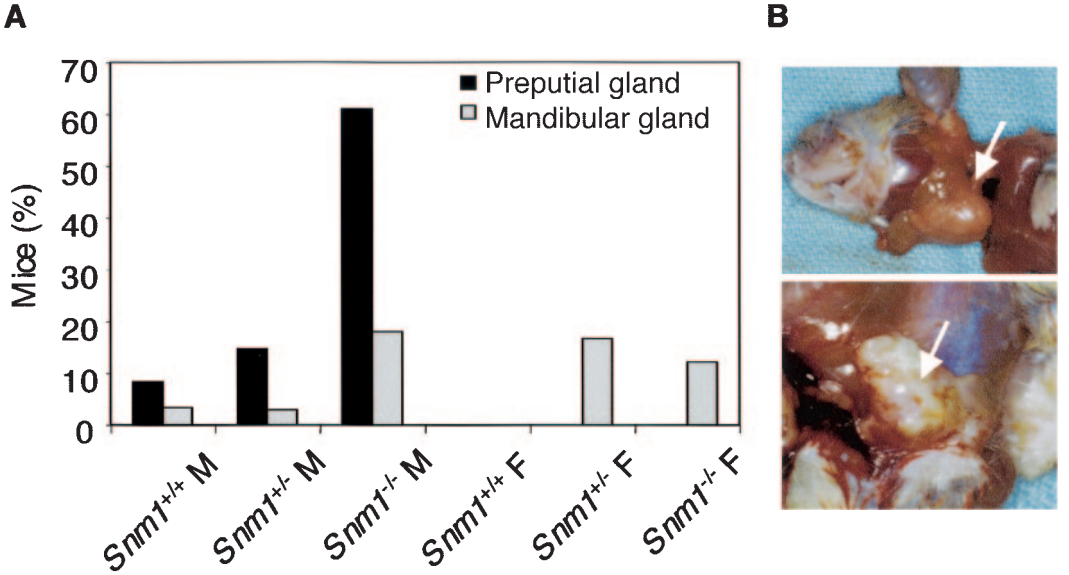

FIG. 3. Incidence of infections in *Snm1* mice. (A) Frequencies of bacterial infections in preputial and mandibular glands of *Snm1* mice up to 24 months of age. (B) Examples (arrows) of infected organs, mandibular gland (upper) and preputial gland (lower), obtained from *Snm1*$^{-/-}$ mice.

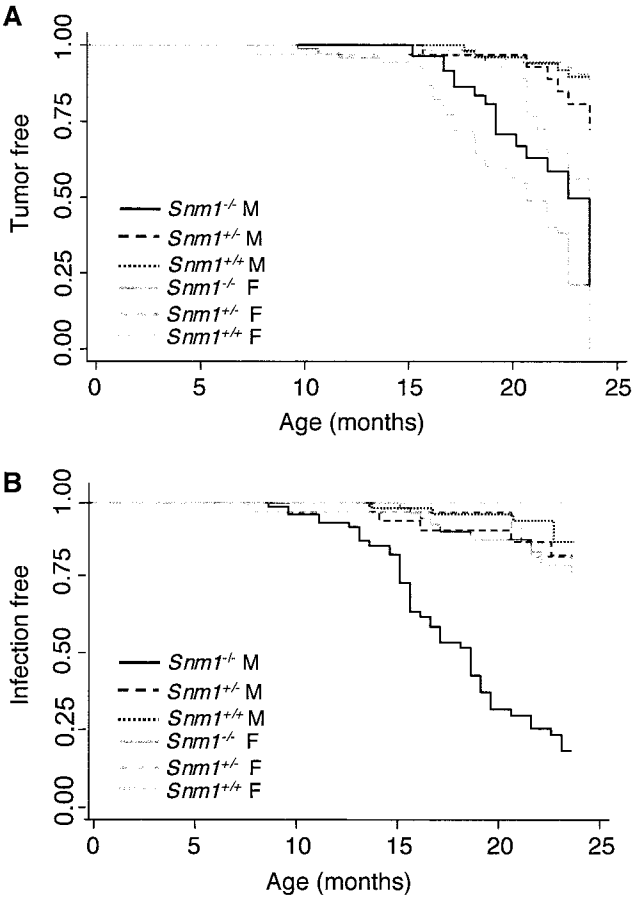

FIG. 4. Effects of infections and tumorigenesis on the mortality of *Snm1* mice. The number of mice within each genotype that were followed for tumor development and infections and the mean risk values are given in Tables 1 and 2, respectively. (A) Kaplan-Meier tumor-free-survival curve by gender and genotype of *Snm1* cohort mice versus age in months. (B) Kaplan-Meier infection-free-survival curve by gender and genotype of *Snm1* cohort mice versus age in months.

Mendelian ratios, were viable and fertile, and did not immediately exhibit an evident phenotype. The mice were observed for a period of 24 months, and both the $Snm1^{-/-}$ and the $Snm1^{+/-}$ mice showed decreased survival compared to wild-type littermates, as indicated by a Kaplan-Meier analysis (Fig. 2A). The differences were statistically significant for both the heterozygous and homozygous mutant mice ($P < 0.001$). The decreased survival was due principally to two identified factors: increased susceptibility to bacterial (*Staphylococcus aureus*) infections and accelerated tumorigenesis. When the animals were analyzed by gender, males showed a reduction in survival compared to females (Fig. 2B), and this difference was due to a greater incidence of infection in the males. Only two sites of infection were noted, namely, the preputial gland and the mandibular gland, with the majority of infections in the male occurring at the former site (Fig. 3). A much lower level of infections was observed in females, and only in the mandibular gland. To determine the relative contributions of infections and tumorigenesis to the mortality of S*nm1* mice, we examined these factors independently. This analysis (Fig. 4A) showed that tumorigenesis was significantly different in both homozygous ($P < 0.001$) and heterogenous ($P < 0.001$) females and in homozygous males ($P < 0.001$) compared to wild-type animals of the same gender (Table 1). Homozygous females were also more prone to tumorigenesis than homozygous males ($P = 0.008$). Infections (Fig. 4B) were significantly more frequent only in the homozygous males compared to the wild-type males ($P < 0.001$) (Table 2).

The types of cancers found in *Snm1* mice were primarily hematologic tumors, with fewer occurrences of adenomas and sarcomas (Table 3). Without any treatment, we monitored heterozygous and homozygous *Snm1*-deficient mice and normal littermates for spontaneous tumor development until 20 months of age. The most common tumors arising spontaneously in these animals were lymphomas. No tumors were observed in wild-type mice (28 animals) until the age of 17 months. From 17 to 20 months of age, four wild-type mice (14.3%) developed lymphoma (systemic or mesenteric lymph node) and one mouse (3.6%) developed a histiocytic sarcoma. Heterozygous *Snm1* mice started to develop tumors from the age of 16 months. Out of 16 mice, 4 heterozygous mice (25%) developed lymphoma (systemic or lung, mandibular, or adrenal lymph node) and 1 mouse (6.3%) developed histiocytic sarcoma. In our study population of homozygous animals, both females (66.66%) and males (28.57%) developed a similar spectrum of tumor types. The first noted occurrence of tumors in the males was at 15 months of age, whereas tumors first appeared in the females at around 11 months of age. Tumor occurrence in female homozygous mice increased significantly at 15 months of age (Fig. 4A). Out of 61 homozygous mice, 24 (39.3%) had lymphoma, with the highest occurrences in the mandibular lymph node, mesenteric lymph node, spleen, liver, or lung or systemically and lesser occurrences in adrenal gland, thymus, kidney, ovaries, mesoderm, bone marrow, or pancreas. Two of 24 mice with lymphoma also developed lung adenoma, and 1 of these 24 animals also developed ovarian cyst ade-

TABLE 1. Tumor susceptibility of mice at 24 months

Genotype, sex	*n*	Risk[a] (%)	*P* value[b]
$SNM1^{+/+}$, male	64	22.2 ± 6.2	
$SNM1^{+/-}$, male	39	27.9 ± 9.0	0.52
$SNM1^{-/-}$, male	85	100	<0.001
$SNM1^{+/+}$, female	60	20.1 ± 5.7	
$SNM1^{+/-}$, female	33	61.2 ± 9.9	<0.001
$SNM1^{-/-}$, female	78	100	<0.001

[a] Risk ± standard error.
[b] Log rank test for equality of tumor development compared with wild type.

TABLE 2. Risk of infection for mice at 24 months

Genotype, sex	*n*	Risk[a] (%)	*P* value[b]
$SNM1^{+/+}$, male	64	12.4 ± 4.8	
$SNM1^{+/-}$, male	39	21.3 ± 7.9	0.12
$SNM1^{-/-}$, male	85	80.0 ± 5.6	<0.001
$SNM1^{+/+}$, female	60	0	
$SNM1^{+/-}$, female	33	23.6 ± 9.6	0.32
$SNM1^{-/-}$, female	78	20.0 ± 7.0	0.12

[a] Risk ± standard error.
[b] Log rank test for equality of infection compared with wild-type male.

TABLE 3. Tumor spectrum in *Snm1* mice[a]

Genotype	Tumor type	Incidence (%)
$Snm1^{-/-}$ ($n = 61$)	Lymphoma	39.3
	Adenoma	9.8
	Cyst adenoma	9.8
	Sarcoma	5.0
	Histiocytic sarcoma	3.3
	Teratoma	1.6
$Snm1^{+/-}$ ($n = 16$)	Lymphoma	25
	Histiocytic sarcoma	6.3
$Snm1^{+/+}$ ($n = 28$)	Lymphoma	14.3
	Histiocytic sarcoma	3.6

[a] Monitored until 20 months of age.

noma. Additionally, two mice (3.3%) had histiocytic sarcoma, three mice (5.0%) had sarcoma (liver), six mice (9.8%) had adenoma (lung and hardarian gland), six mice (9.8%) had cyst adenoma (ovary, uterus, and papillary hardarian gland), and one mouse had malignant teratoma (ovary). All tumors were analyzed in detail by histopathology (Fig. 5). We conclude that *Snm1* mice are susceptible to accelerated tumorigenesis and that the incidence is greater in females than in males.

***Snm1* mice have normal T- and B-cell development and immunoglobulin class switch recombination.** As noted above (Fig. 3), the frequency of infections, particularly in the $Snm1^{-/-}$ male mice, was extremely high, with almost 80% of these animals exhibiting the condition between 10 and 24 months of age. The vast majority of these infections occurred in the preputial gland, indicating that this organ in the male was particularly susceptible. To assess for a possible immunological dysfunction in $Snm1^{-/-}$ mice, we analyzed the levels of T and B lymphocytes. As shown (see Fig. S1 in the supplemental material), T and B lymphocytes were grossly normal in $Snm1^{-/-}$ mice compared to wild-type littermates. We found that total thymocyte numbers in $Snm1^{-/-}$ mice were very similar to those in wild-type mice and that CD4/CD8 double- or single-positive populations were comparable to those found in wild-type animals. Both $CD4^+$ and $CD8^+$ T cells are normal in peripheral blood (see Fig. S1A in the supplemental material). Similar results were obtained in the B-lymphocyte compartment. We checked bone marrow, spleen, and lymph nodes and found no differences in FACS profiles between $Snm1^{-/-}$ and wild-type mice (see Fig. S1B in the supplemental material). Based on these observations, we conclude that *Snm1*, unlike its family member *Artemis*, is not required for V(D)J recombination.

To determine if $Snm1^{-/-}$ B cells are able to undergo CSR, we first examined the level of serum immunoglobulin isotypes of $Snm1^{-/-}$ and wild-type mice by a flow cytometry assay using FITC- and PE-based beads. Our results showed that all isotypes examined were present in both male and female $Snm1^{-/-}$ mice (data not shown), indicating that *Snm1* is not required for CSR.

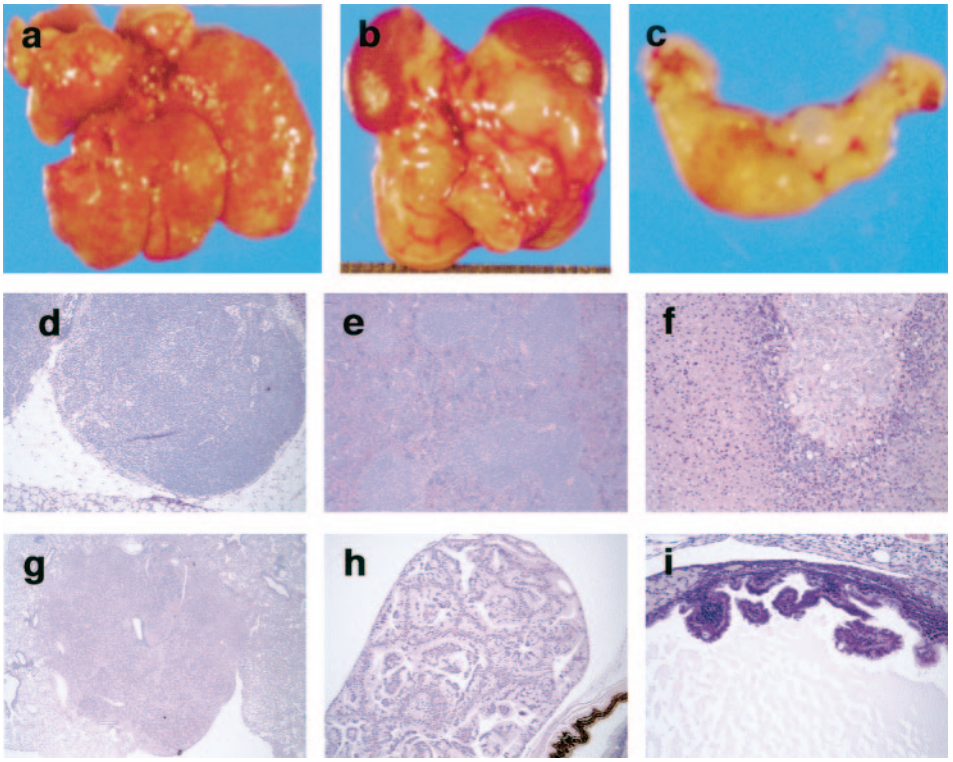

FIG. 5. Histologic analysis of tumors found in $Snm1^{-/-}$ mice. (a to c) Examples of spontaneous tumors from different organs of $Snm1^{-/-}$ mice: (a) liver, (b) adrenal gland, and (c) uterus and ovary. (d to f) Representative histology of lymphomas of $Snm1^{-/-}$ mice: (d) mandibular lymph node lymphoma, ×100 magnification; (e) spleen lymphoma, ×50 magnification; and (f) adrenal gland lymphoma, ×200 magnification. (g to i) Representative histology of adenomas of $Snm1^{-/-}$ mice: (g) lung adenoma, ×20 magnification; (h) papillary hardarian gland adenoma, ×50 magnification; and (i) ovary cyst adenoma, ×200 magnification. All tumors were obtained from 15-month- to 20-month-old $Snm1^{-/-}$ mice. The tissues were paraffin embedded and stained with hematoxylin and eosin stain.

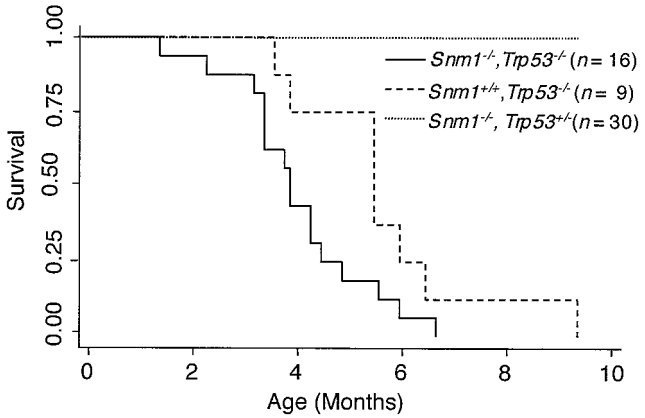

FIG. 6. Homozygosity for *Snm1* decreases the survival of $Trp53^{-/-}$ mice. Kaplan-Meier analysis showing the survival of $Snm1^{-/-}$ $Trp53^{-/-}$, $Snm1^{+/+}$ $Trp53^{-/-}$, and $Snm1^{-/-}$ $Trp53^{+/-}$ cohort mice versus age in months.

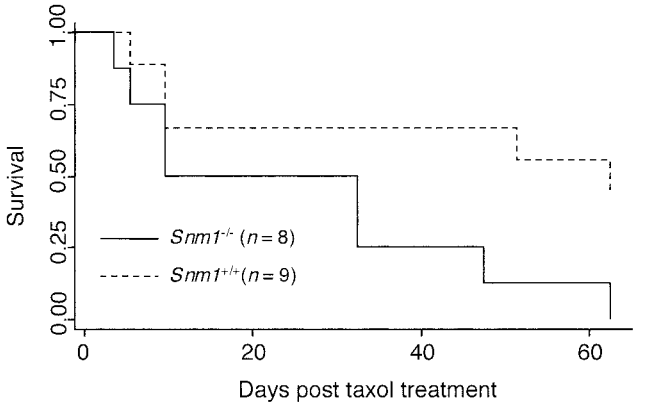

FIG. 7. *Snm1* homozygous mice are hypersensitive to the spindle poison taxol. Kaplan-Meier analysis showing the survival of $Snm1^{-/-}$ and $Snm1^{+/+}$ mice versus age after injection of taxol at 15 mg/kg of body weight.

To confirm that $Snm1^{-/-}$ B cells are able to undergo class switch recombination, we stimulated in vitro cultures of splenocytes from mutant and wild-type mice (18). The results demonstrated that splenocytes from $Snm1^{-/-}$ mice underwent CSR normally after lipopolysaccharide or interleukin-4/CD40 stimulation (data not shown). Therefore, both in vivo and in vitro analyses indicated that *Snm1* mutant mice are able to undergo class switching, and we conclude that *Snm1* is not essential for CSR.

***Snm1* deficiency accelerates tumorigenesis in *Trp53* null mice.** A number of studies have shown cooperation between a potential tumor suppressor gene and *Trp53* (3, 7, 24, 34). Thus, to further assess the tumor suppression activity of *Snm1*, we derived $Snm1^{+/-}$ $Trp53^{+/-}$ mice and then bred progeny. All genotypes were born at Mendelian frequency and appeared normal at birth. However, we observed a statistically significant decrease in the survival of $Snm1^{-/-}$ $Trp53^{-/-}$ mice compared to $Snm1^{+/+}$ $Trp53^{-/-}$ littermates ($P = 0.05$) (Fig. 6). The time to 50% survival was approximately 4 months for the former mice compared to 5.5 months for the latter mice. Histological analysis indicated that 100% of the $Snm1^{-/-}$ $Trp^{-/-}$ mice had developed thymic lymphomas, and a majority of these animals had also developed nonthymic lymphomas (Table 4). Sarcomas were not observed in any of the 14 $Snm1^{-/-}$ $Trp^{-/-}$ mice, whereas sarcomas were observed in $Snm1^{+/-}$ $Trp^{-/-}$ mice.

***Snm1* mice are hypersensitive to taxol.** As indicated in the introduction, $Snm1^{-/-}$ MEFs are highly sensitive to spindle poisons, such as nocodazole and taxol (1). To determine the effects of a spindle poison on whole animals, we injected wild-type and homozygous mice with a single dose of taxol (15 mg/kg of body weight) and subsequently monitored the animals for morbidity. By 64 days, all of the $Snm1^{-/-}$ mice had died compared to approximately 50% of the wild-type mice ($P = 0.0282$) (Fig. 7). These findings are consistent with our previous observations of hypersensitivity to spindle poisons in $Snm1^{-/-}$ MEFs. We have also found that human Snm1 localizes to sites of DSBs after exposure of cells to IR (23); however, Dronkert et al. (9) have reported that $Snm1^{-/-}$ ES cells do not exhibit hypersensitivity to IR. To determine the IR sensitivity of whole animals, we irradiated wild-type and homozygous mice with 7.5 Gy; however, no statistically significant difference in survival between the two genotypes was observed (results not shown).

***Snm1* MEFs exhibit a proliferation defect in culture.** To examine the effects of *Snm1* deficiency at the cellular level, embryonic fibroblasts (MEFs) were prepared from 13.5-day embryos and examined by the 3T3 proliferation protocol (30). As shown in Fig. S2 in the supplemental material, MEFs derived from homozygous mice exhibited a profound proliferation defect at all passages examined compared to wild-type MEFs. These results indicate that under tissue culture conditions *Snm1* has a role in normal cell growth. Upon spontaneous immortalization, both mutant and wild-type MEFs grew at approximately equal rates. Finally, as indicated above, a previous report showed that $Snm1^{-/-}$ ES cells exhibit an approximately twofold hypersensitivity to MMC and no demonstrable sensitivity to IR compared to wild-type cells (9). We performed similar experiments with the *Snm1* MEFs and essentially confirmed these findings, i.e., no hypersensitivity to IR and a small hypersensitivity to MMC (see Fig. S3 in the supplemental material).

TABLE 4. Tumor types in *Trp531Snm1* mice

Tumor type	No. (%) in $Trp53^{-/-}$ mice		
	$Snm1^{-/-}$ ($n = 14$)	$Snm1^{+/-}$ ($n = 15$)	$Snm1^{+/+}$ ($n = 8$)
Lymphoma			
Thymic	14 (100)	8 (53.3)	3 (37.5)
Nonthymic	9 (64.3)	7 (46.7)	4 (50)
Sarcoma			
Soft tissue	0 (0)	3 (18.8)	3 (37.5)
Osteosarcoma	0 (0)	2 (12.5)	1 (12.5)

DISCUSSION

Our studies of *Snm1* knockout mice have revealed an involvement of this gene in the suppression of spontaneous tumorigenesis and in mediating resistance to infection. The latter

function was found to be statistically significant only in male animals, principally due to the location of the infections in the preputial gland. This gland occurs in both males and females but is anatomically quite distinct between the two genders. The basis for the presumed immunodeficiency remains unresolved, as analyses of T- and B-cell development did not indicate any defects in these processes. Since *Snm1* is a member of the gene family that includes *Artemis*, an involvement in immune function seemed a possibility. *Artemis* deficiency results in a SCID syndrome in which mature T and B cells fail to develop due to impaired V(D)J rearrangements at T-cell receptor and immunoglobulin genes (19, 25). Our analyses of *Snm1*$^{-/-}$ mice clearly indicated that *Snm1* is not involved in V(D)J recombination. Additionally, we showed previously that human Snm1 interacts with 53BP1 (23), and *Trp53bp1* mutant mice have been shown to be critical for immunoglobulin class switch recombination (18). Our results demonstrated that *Snm1* is not essential for CSR, since both male and female *Snm1*-deficient mice are able to undergo CSR. It is also possible that the *Snm1* deficiency may lead to a defect in innate immunity against certain bacterial infections. While the nature of the immune dysfunction remains unsettled, it is clear that it contributes significantly to the mortality of the male homozygous mutant mice.

Snm1 is the third member of the mammalian SNM1 gene family to be implicated as a tumor suppressor. In a genome-wide screen of high-risk pedigrees, mutations in *ELAC2*/*HPC2* were found to segregate with prostate cancer (29). *ELAC2* is a gene of unknown function whose risk genotypes have been estimated to cause approximately 2% of prostate cancer in the general population (5); however, other studies have not found such a definitive role for *ELAC2* in this disease (27). Disruption of *Artemis* in the mouse confirmed the SCID phenotype but did not indicate any accelerated tumorigenesis in the knockout animals (25). However, when these mice were crossed with *Trp53*-deficient animals, a marked and early-onset predisposition to progenitor B-cell lymphomas was observed, indicating that *Artemis* is a tumor suppressor (24). *Artemis*-deficient cells exhibit genomic instability, which may be due to a defect in the NHEJ pathway of DSB repair or in cell cycle regulation (15, 22, 33). A previous study of a disruption of *Snm1* in the mouse did not report any evidence of accelerated tumorigenesis in these animals (9). While other explanations are possible, the most likely reason for the discrepancy is that the targeted gene strategy used in that study resulted in disruption of only a portion of intron 3 and 25 amino acids of exon 4. In addition, PCR analysis indicated that transcripts produced by the use of an alternative splice site in exon 5 restored the reading frame. Thus, it is possible that the previously reported *Snm1* knockout represents a hypomorphic rather than a null allele.

Our previous studies have defined a role for *Snm1* in an early mitotic checkpoint that arrests cells in response to spindle poisons, such as nocodazole and taxol (1). This checkpoint occurs in prophase before the onset of chromosome condensation. The phenotype of *Snm1*-deficient cells is highly comparable to the phenotype of *Chfr*-deficient cells in that both appear defective in a prophase checkpoint in response to spindle poisons (28). *Chfr* was found to be mutated in about half of human cancer cell lines examined (28), and furthermore, in a recent report a knockout of *Chfr* in the mouse indicated that it had a strong tumor suppression function (31). Both *Snm1*- and *Chfr*-deficient cells have a marked hypersensitivity to spindle poisons, consistent with a defect in the prophase checkpoint. Our findings reported here confirm these results by demonstrating that *Snm1* homozygous animals exhibit increased mortality compared to wild-type mice upon injection of taxol. Taken together, these findings indicate that the prophase checkpoint pathway plays an important role in tumor suppression.

Yeast *Snm1* mutants are highly and singularly sensitive to interstrand cross-linking agents (10, 26), however, a specific role for mammalian *Snm1* in DNA cross-link repair seems unlikely. Mouse ES cells disrupted in *Snm1* showed slight hypersensitivity to MMC, but not to the cross-linking agent melphalan or psoralen plus UVA (9), and our findings indicated only a slight hypersensitivity to MMC in MEFs. One suggested possibility to account for this result is that there is redundancy among the *SNM1* family members in DNA repair pathways. However, outside of the SNM1 domain, the mammalian family members show no sequence conservation. Additionally, *Artemis*-deficient cells exhibit no sensitivity to cross-linking agents (19, 25), and small interfering RNA depletion of Snm1B revealed only minor sensitivity to cisplatin or MMC (8). These results suggest that while *SNM1* genes have a role in the stress response to genotoxic agents, they are unlikely to have a direct role in the repair of DNA interstrand cross-links.

In summary, our findings provide the first genetic model demonstrating the role of *Snm1* as a tumor suppressor gene in mice. We have also demonstrated that *Snm1* has a role in immunity, although the nature of this function and why it is particularly important in the male preputial gland remain to be resolved.

ACKNOWLEDGMENTS

This work was supported by NCI grants CA52461, CA96574, and CA90270; EHS grant ES07784; The Leukemia Research Foundation; and a UT M. D. Anderson Institutional Grant (C.Z.). DNA sequencing and veterinary resources were supported by Cancer Center Support (Core) Grant CA16672.

REFERENCES

1. **Akhter, S., C. T. Richie, J. M. Deng, E. Brey, X. Zhang, C. Patrick, Jr., R. R. Behringer, and R. J. Legerski.** 2004. Deficiency in SNM1 abolishes an early mitotic checkpoint induced by spindle stress. Mol. Cell. Biol. **24:** 10448–10455.
2. **Barber, L. J., T. A. Ward, J. A. Hartley, and P. J. McHugh.** 2005. DNA interstrand cross-link repair in the *Saccharomyces cerevisiae* cell cycle: overlapping roles for PSO2 (SNM1) with MutS factors and EXO1 during S phase. Mol. Cell. Biol. **25:**2297–2309.
3. **Bassing, C. H., H. Suh, D. O. Ferguson, K. F. Chua, J. Manis, M. Eckersdorff, M. Gleason, R. Bronson, C. Lee, and F. W. Alt.** 2003. Histone H2AX: a dosage-dependent suppressor of oncogenic translocations and tumors. Cell **114:**359–370.
4. **Callebaut, I., D. Moshous, J. P. Mornon, and J. P. de Villartay.** 2002. Metallo-beta-lactamase fold within nucleic acids processing enzymes: the beta-CASP family. Nucleic Acids Res. **30:**3592–3601.
5. **Camp, N. J., and S. V. Tavtigian.** 2002. Meta-analysis of associations of the Ser217Leu and Ala541Thr variants in ELAC2 (HPC2) and prostate cancer. Am. J. Hum. Genet. **71:**1475–1478.
6. **Cavazzana-Calvo, M., F. Le Deist, G. De Saint Basile, D. Papadopoulo, J. P. De Villartay, and A. Fischer.** 1993. Increased radiosensitivity of granulocyte macrophage colony-forming units and skin fibroblasts in human autosomal recessive severe combined immunodeficiency. J. Clin. Investig. **91:**1214–1218.
7. **Celeste, A., S. Difilippantonio, M. J. Difilippantonio, O. Fernandez-Capetillo, D. R. Pilch, O. A. Sedelnikova, M. Eckhaus, T. Ried, W. M. Bonner, and A. Nussenzweig.** 2003. H2AX haploinsufficiency modifies genomic stability and tumor susceptibility. Cell **114:**371–383.

8. **Demuth, I., M. Digweed, and P. Concannon.** 2004. Human SNM1B is required for normal cellular response to both DNA interstrand crosslink-inducing agents and ionizing radiation. Oncogene **23:**8611–8618.
9. **Dronkert, M. L., J. de Wit, M. Boeve, M. L. Vasconcelos, H. van Steeg, T. L. Tan, J. H. Hoeijmakers, and R. Kanaar.** 2000. Disruption of mouse SNM1 causes increased sensitivity to the DNA interstrand cross-linking agent mitomycin C. Mol. Cell. Biol. **20:**4553–4561.
10. **Henriques, J. A., and E. Moustacchi.** 1980. Isolation and characterization of pso mutants sensitive to photo-addition of psoralen derivatives in *Saccharomyces cerevisiae*. Genetics **95:**273–288.
11. **Horan, G. S., E. N. Kovacs, R. R. Behringer, and M. S. Featherstone.** 1995. Mutations in paralogous Hox genes result in overlapping homeotic transformations of the axial skeleton: evidence for unique and redundant function. Dev. Biol. **169:**359–372.
12. **Jacks, T., L. Remington, B. O. Williams, E. M. Schmitt, S. Halachmi, R. T. Bronson, and R. A. Weinberg.** 1994. Tumor spectrum analysis in p53-mutant mice. Curr. Biol. **4:**1–7.
13. **Jenny, A., L. Minvielle-Sebastia, P. J. Preker, and W. Keller.** 1996. Sequence similarity between the 73-kilodalton protein of mammalian CPSF and a subunit of yeast polyadenylation factor I. Science **274:**1514–1517.
14. **Li, X., J. Hejna, and R. E. Moses.** 2005. The yeast Snm1 protein is a DNA 5′-exonuclease. DNA Repair **4:**163–170.
15. **Ma, Y., H. Lu, B. Tippin, M. F. Goodman, N. Shimazaki, O. Koiwai, C. L. Hsieh, K. Schwarz, and M. R. Lieber.** 2004. A biochemically defined system for mammalian nonhomologous DNA end joining. Mol. Cell **16:**701–713.
16. **Ma, Y., U. Pannicke, K. Schwarz, and M. R. Lieber.** 2002. Hairpin opening and overhang processing by an Artemis/DNA-dependent protein kinase complex in nonhomologous end joining and V(D)J. recombination. Cell **108:**781–794.
17. **Magana-Schwencke, N., J. A. Henriques, R. Chanet, and E. Moustacchi.** 1982. The fate of 8-methoxypsoralen photoinduced crosslinks in nuclear and mitochondrial yeast DNA: comparison of wild-type and repair-deficient strains. Proc. Natl. Acad. Sci. USA **79:**1722–1726.
18. **Manis, J. P., J. C. Morales, Z. Xia, J. L. Kutok, F. W. Alt, and P. B. Carpenter.** 2004. 53BP1 links DNA damage-response pathways to immunoglobulin heavy chain class-switch recombination. Nat. Immunol. **5:**481–487.
19. **Moshous, D., I. Callebaut, R. de Chasseval, B. Corneo, M. Cavazzana-Calvo, F. Le Deist, I. Tezcan, O. Sanal, Y. Bertrand, N. Philippe, A. Fischer, and J. P. de Villartay.** 2001. Artemis, a novel DNA double-strand break repair/V(D)J recombination protein, is mutated in human severe combined immune deficiency. Cell **105:**177–186.
20. **Moshous, D., L. Li, R. Chasseval, N. Philippe, N. Jabado, M. J. Cowan, A. Fischer, and J. P. de Villartay.** 2000. A new gene involved in DNA double-strand break repair and V(D)J recombination is located on human chromosome 10p. Hum. Mol. Genet. **9:**583–588.
21. **Nicolas, N., D. Moshous, M. Cavazzana-Calvo, D. Papadopoulo, R. de Chasseval, F. Le Deist, A. Fischer, and J. P. de Villartay.** 1998. A human severe combined immunodeficiency (SCID) condition with increased sensitivity to ionizing radiations and impaired V(D)J rearrangements defines a new DNA recombination/repair deficiency. J. Exp. Med. **188:**627–634.
22. **Riballo, E., M. Kuhne, N. Rief, A. Doherty, G. C. Smith, M. J. Recio, C. Reis, K. Dahm, A. Fricke, A. Krempler, A. R. Parker, S. P. Jackson, A. Gennery, P. A. Jeggo, and M. Lobrich.** 2004. A pathway of double-strand break rejoining dependent upon ATM, Artemis, and proteins locating to gamma-H2AX foci. Mol. Cell **16:**715–724.
23. **Richie, C. T., C. Peterson, T. Lu, W. N. Hittelman, P. B. Carpenter, and R. J. Legerski.** 2002. hSnm1 colocalizes and physically associates with 53BP1 before and after DNA damage. Mol. Cell. Biol. **22:**8635–8647.
24. **Rooney, S., J. Sekiguchi, S. Whitlow, M. Eckersdorff, J. P. Manis, C. Lee, D. O. Ferguson, and F. W. Alt.** 2004. Artemis and p53 cooperate to suppress oncogenic N-myc amplification in progenitor B cells. Proc. Natl. Acad. Sci. USA **101:**2410–2415.
25. **Rooney, S., J. Sekiguchi, C. Zhu, H. L. Cheng, J. Manis, S. Whitlow, J. DeVido, D. Foy, J. Chaudhuri, D. Lombard, and F. W. Alt.** 2002. Leaky Scid phenotype associated with defective V(D)J coding end processing in Artemis-deficient mice. Mol. Cell **10:**1379–1390.
26. **Ruhland, A., M. Kircher, F. Wilborn, and M. Brendel.** 1981. A yeast mutant specifically sensitive to bifunctional alkylation. Mutat. Res. **91:**457–462.
27. **Schaid, D. J.** 2004. The complex genetic epidemiology of prostate cancer. Hum. Mol. Genet. **13:**R103–R121.
28. **Scolnick, D. M., and T. D. Halazonetis.** 2000. Chfr defines a mitotic stress checkpoint that delays entry into metaphase. Nature **406:**430–435.
29. **Tavtigian, S. V., J. Simard, D. H. Teng, V. Abtin, M. Baumgard, A. Beck, N. J. Camp, A. R. Carillo, Y. Chen, P. Dayananth, M. Desrochers, M. Dumont, J. M. Farnham, D. Frank, C. Frye, S. Ghaffari, J. S. Gupte, R. Hu, D. Iliev, T. Janecki, E. N. Kort, K. E. Laity, A. Leavitt, G. Leblanc, J. McArthur-Morrison, A. Pederson, B. Penn, K. T. Peterson, J. E. Reid, S. Richards, M. Schroeder, R. Smith, S. C. Snyder, B. Swedlund, J. Swensen, A. Thomas, M. Tranchant, A. M. Woodland, F. Labrie, M. H. Skolnick, S. Neuhausen, J. Rommens, and L. A. Cannon-Albright.** 2001. A candidate prostate cancer susceptibility gene at chromosome 17p. Nat. Genet. **27:**172–180.
30. **Todaro, G. J., and H. Green.** 1963. Quantitative studies of the growth of mouse embryo cells in culture and their development into established lines. J. Cell Biol. **17:**299–313.
31. **Yu, X., K. Minter-Dykhouse, L. Malureanu, W. M. Zhao, D. Zhang, C. J. Merkle, I. M. Ward, H. Saya, G. Fang, J. van Deursen, and J. Chen.** 2005. Chfr is required for tumor suppression and Aurora A regulation. Nat. Genet. **37:**401–406.
32. **Zhang, X., C. Richie, and R. J. Legerski.** 2002. Translation of hSNM1 is mediated by an internal ribosome entry site that upregulates expression during mitosis. DNA Repair **1:**379–390.
33. **Zhang, X., J. Succi, Z. Feng, S. Prithivirajsingh, M. D. Story, and R. J. Legerski.** 2004. Artemis is a phosphorylation target of ATM and ATR and is involved in the G_2/M DNA damage checkpoint response. Mol. Cell. Biol. **24:**9207–9220.
34. **Zhu, C., K. D. Mills, D. O. Ferguson, C. Lee, J. Manis, J. Fleming, Y. Gao, C. C. Morton, and F. W. Alt.** 2002. Unrepaired DNA breaks in p53-deficient cells lead to oncogenic gene amplification subsequent to translocations. Cell **109:**811–821.